Cytochromes c_{555} from the Hyperthermophilic Bacterium *Aquifex aeolicus* (VF5). 1. Characterization of Two Highly Homologous, Soluble and Membranous, Cytochromes c_{555}[†]

Frauke Baymann,[‡] Pascale Tron,[‡] Barbara Schoepp-Cothenet,*[,‡] Corinne Aubert,[‡] Pierre Bianco,[‡] Karl-Otto Stetter,[§] Wolfgang Nitschke,[‡] and Michael Schütz[‡,||]

Laboratoire de Bioénergétique et Ingénierie des Protéines (UPR9036), CNRS, 31 chemin Joseph Aiguier, F-13402 Marseille Cedex 20, France, and Lehrstuhl für Mikrobiologie und Archaeenzentrum, Universität Regensburg, Universitätsstrasse 31, D-93040 Regensburg, Germany

Received June 11, 2001; Revised Manuscript Received August 13, 2001

ABSTRACT: Two distinct class I (monoheme) *c*-type cytochromes from the hyperthermophilic bacterium *Aquifex aeolicus* were studied by biochemical and biophysical methods (i.e., optical and EPR spectroscopy, electrochemistry). The sequences of these two heme proteins (encoded by the *cyc*B1 and *cyc*B2 genes) are close to identical (85% identity in the common part of the protein) apart from the presence of an N-terminal stretch of 62 amino acid residues present only in the *cyc*B1 gene. A soluble cytochrome was purified and identified by N-terminal sequencing as the *cyc*B2 gene product. It showed an α-peak at 555 nm, an E_m value of +220 mV, and electron paramagnetic resonance parameters of $g_z = 2.89$, $g_y = 2.287$, and $g_x = 1.52$. A firmly membrane-bound cytochrome characterized by nearly identical properties was detected and attributed to the *cyc*B1 gene product. The very high degree of homology of its N-terminal part to cytochrome c_{553} from *Heliobacterium gestii* strongly suggests it to be anchored to the membrane via N-terminally attached lipid molecules. The two heme proteins were named cytochrome c_{555}^{s} (soluble) and cytochrome c_{555}^{m} (membranous). Electron paramagnetic resonance on partially ordered membrane multilayers suggests that the solvent-exposed heme domain of cytochrome c_{555}^{m} is flexible with respect to the membrane plane. Possible functional roles for both cytochromes are discussed.

The hyperthermophilic chemotroph *Aquifex aeolicus* (*1*) is a member of the Aquificales, considered to represent the earliest branching order of the phylogenetic tree of the Bacteria (*2*). *A. aeolicus* has been the target of a genome sequencing project achieved in 1998 (*3*) and has then entered the early proteomics era marked by an abundance of genomic information confronted by a scarcity of data with respect to metabolic mechanisms and functional/structural properties of enzymes involved.

Recently, several components of the electron transfer chain in *A. aeolicus* have been studied. The structure of a soluble ferredoxin has been solved (*4*), the sulfide:quinone oxidoreductase (SQR) has been characterized in membranes (*5*), the [Ni/Fe] hydrogenases have been purified and studied with respect to functional properties and phylogenetic positioning (Guiral et al., unpublished data), and analysis of the cytochrome *bc* complex in membranes and partially purified isolates is underway (Schütz et al., unpublished data). A detailed phylogenetic analysis of cytochrome *bc*-type enzymes (*6*) has recently shown that the enzyme from *Aquifex* is phylogenetically closely related to its homologue in the ϵ-proteobacteria *Helicobacter pylori* and *Campylobacter jejuni*, reminiscent of reports on a number of other proteins from this organism which were also found to be close to their proteobacterial counterparts with respect to amino acid sequence (*7*). On the basis of an inspection of the genomic environment of the genes coding for the *bc* complex in *Aquifex*, it was concluded that this species most probably has experienced extensive donation of genes from an ϵ-proteobacterium (*6*). A more detailed analysis of the open reading frames in the *Aquifex* genome indicated that about 20% of identifiable genes are close to ϵ-proteobacterial homologues, whereas the remaining 80% are strongly related to proteins from *Thermotoga*, *Deinococcus*, *Thermus*, and Archaea (Brugna and Nitschke, unpublished data), i.e., in line with the positioning of the species by 16S rRNA (*8*) and whole genome analysis (*9*).

In this work, we describe the biochemical and physicochemical properties of a soluble and a membrane-attached cytochrome, highly homologous to each other. We compare the amino acid sequences of both cytochromes to those of homologous proteins from other species and discuss their possible functional roles.

MATERIALS AND METHODS

Bacterial Culture Conditions, Membrane Preparation, and Cytochrome Purification. *A. aeolicus* (VF5) was grown, and

[†] The work of K.-O.S. was financially supported by the Fonds der Chemischen Industrie, and the project on *Aquifex* at the BIP in Marseille benefited from financial support by the PCV program of the CNRS.

* To whom correspondence should be addressed. Tel: +33 4 91164672. Fax: +33 4 91164578. E-mail: schoepp@ibsm.cnrs-mrs.fr.

[‡] Laboratoire de Bioénergétique et Ingénierie des Protéines (UPR9036), CNRS.

[§] Lehrstuhl für Mikrobiologie und Archaeenzentrum, Universität Regensburg.

[||] Present address: PROFOS AG, Regensburg, Germany.

10.1021/bi011201y CCC: $20.00
Published on Web 10/13/2001

cells were harvested as described previously (*1*). Membranes were prepared according to Nübel et al. (*5*). When indicated, the membrane fraction was ultrasonicated in the presence of 2 M sodium bromide, stirred on ice for 1 h, and centrifuged for 1 h at 200000*g* in order to eliminate weakly membrane-attached proteins. For the purification of soluble cytochrome c_{555}, cells were resuspended in 50 mM Hepes/NaOH, pH 7, 4 mM $MgCl_2$, 0.5 mM PMSF,[1] and 10 μg/mL DNase. The soluble fraction was loaded on a DEAE-cellulose column equilibrated with a buffer containing 50 mM Hepes/NaOH, pH 7, 5 mM EDTA, and 0.5 mM PMSF. The unretained fraction was subsequently applied onto a hydroxylapatite Bio-Gel column, and cytochrome $c_{555}{}^{s}$ was eluted at 50 mM sodium phosphate buffer, pH 7.0. All purification steps were performed at room temperature.

Optical and Electron Paramagnetic Resonance Spectroscopy. Optical spectra were recorded on an Aminco DW-2 spectrophotometer (SLM Instruments Inc., Urbana, IL); electron paramagnetic resonance (EPR) spectra were obtained using a Bruker ESP300e X-band spectrometer fitted with an Oxford Instrument He-cryostat and temperature control system. EPR redox titrations were performed as described by Dutton (*10*) in a buffer containing 50 mM MOPS, pH 7.0, 2 mM EDTA, and 40 mM NaCl in the presence of the following mediators at 100 μM: *N*,*N*,*N*′,*N*′-tetramethyl-*p*-phenylenediamine (TMPD), dichlorophenolindophenol (DCPIP), 2,5-dimethyl-*p*-benzoquinone, 2-hydroxy-1,2-naphthoquinone, cresyl blue, methylene blue, 2,5-dihydroxy-*p*-benzoquinone, indigo carmine, anthraquinone-2,4-disulfonate, anthraquinone-2-sulfonate, safranine T, and neutral red. Ferricyanide was present at 10 μM. Reductive titrations were carried out using sodium dithionite, and oxidative titrations were carried out using ferricyanide and potassium hexachloroiridate(IV). Optical redox titrations of purified soluble cytochrome $c_{555}{}^{s}$ at 20 and 60 °C were performed electrochemically without addition of mediators as described previously (*11*).

Oriented membrane multilayers were produced by partial dehydration in a humidity-controlled atmosphere (*12*, *13*).

Electrochemical Technique. Cyclic (CV) and square-wave (SWV) voltammetries (*14*) with a membrane-working electrode (*15*) were carried out using an EG&G 273A potentiostat controlled by EG&G PAR M 270/250 software. The CV scan rate generally was 20 mV s^{-1}. SWV curves were obtained using 5 Hz as the square-wave frequency, 2 mV as the scan increment, and 25 mV as the pulse height amplitude. A conventional three-electrode system was used in 20 mM deoxygenated phosphate buffer, pH 7. Measurements at room temperature (23 °C) were performed using a polished basal plane pyrolytic graphite electrode. Experiments at higher temperatures required the use of gold electrodes pretreated for 1 min with 1 mM bis(4-pyridyl) disulfide solution (as proposed in ref *16*). The reference electrode was a Metrohm Ag/AgCl/saturated NaCl electrode. The auxiliary electrode was a gold wire.

The pH dependence of the redox midpoint potential was studied in a mixture of three buffer solutions composed of 10 mM sodium acetate/10 mM Tris chloride/10 mM sodium borate adjusted to the required pH. The temperature dependence of the redox midpoint potential was studied in the nonisothermal configuration as proposed in ref *17*.

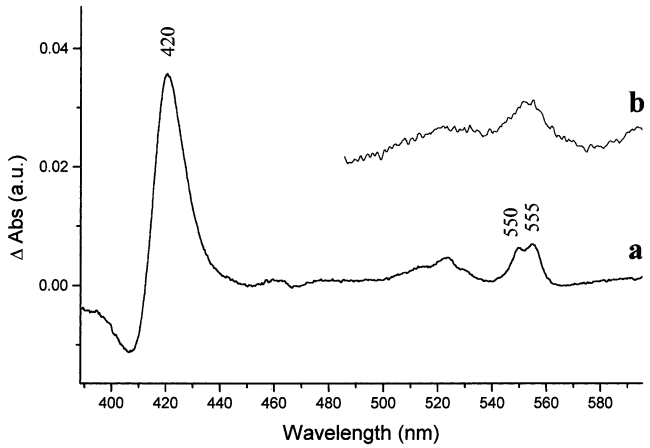

FIGURE 1: Optical absorption difference (ascorbate reduced minus oxidized) spectra of the two cytochromes c_{555} from *A. aeolicus* recorded on the soluble fraction (representing cytochrome $c_{555}{}^{s}$, a) and on membrane fragments (representing cytochrome $c_{555}{}^{m}$, b).

Electrophoretic Analysis. SDS−PAGE was carried out according to the method of Laemmli (*18*). The gels were stained either with Coomassie Blue G-250 or with 3,3′,5,5′-tetramethylbenzidine (TMBZ) as described by Thomas et al. (*19*). N-Terminal protein sequencing was carried out on the apoprotein with an Applied Biosystems gas-phase sequenator (models 470A and 473A).

Sequence Analysis and Structural Models. Database searches for amino acid sequences were performed by BLASTP (*20*) with the amino acid sequence database at the National Center for Biotechnology Information, Washington, DC, or the TIGR microbiology database. The amino acid sequences were aligned with the help of the program CLUSTAL (*21*). Structural models of CycB2 from *A. aeolicus*, using cytochrome c_{552} from *Thermus thermophilus* as template, were obtained using Swiss-Model (*22*).

All chemicals were of reagent grade and were purchased from commercial sources.

RESULTS

Identification of the Cytochromes c_{555}

CycB2 was purified to homogeneity from the soluble fraction of disrupted *A. aeolicus* cells. Absorption difference spectra of the ascorbate-reduced cytochrome are shown in Figure 1, curve a. At 20 °C, reduced cytochrome CycB2's α-band is split, with maxima at 555 and 550 nm. At variance with these spectral data, CycB2 is annotated as cytochrome c_{552} in the *Aquifex* genome. We therefore propose to rename CycB2 as cytochrome $c_{555}{}^{s}$ ("s" standing for "soluble").

SDS−PAGE of the purified cytochrome, after staining with Coomassie Blue as well as with TMBZ (data not shown), shows a single band at approximately 9 kDa revealing a cytochrome with covalently attached heme as is typical for *c*-type cytochromes. The N-terminal peptide sequence of the heme-staining band was determined (ADGKAIFQQK). A BLAST search of this sequence in the *A. aeolicus* genome (*3*) (using the NCBI-genome server)

[1] Abbreviations: DEAE, diethylaminoethyl; EDTA, ethylenediaminetetraacetic acid; E_m, redox midpoint potential; $E_{m,7}$, E_m at pH 7.0; EPR, electron paramagnetic resonance; MOPS, 3′-(*N*-morpholino)propanesulfonic acid; PMSF, phenylmethanesulfonyl fluoride; SDS−PAGE, sodium dodecyl sulfate−polyacrylamide gel electrophoresis.

FIGURE 2: Sequence alignment of cytochrome c_{555}^{s} (Accession Number: F70434; GI7430463) and c_{555}^{m} (B70369; GI7430462) from *A. aeolicus*, cytochrome c_{553} (AAC16774) from *H. gestii*, cytochrome c_{552} (S32485; GI479146) from *H. thermophilus*, cytochrome c_{552} (CCPS5S; GI65547) from *Pseudomonas stutzeri*, and cytochrome c_{554} (AAB88580; GI155079) from *T. thermophilus*. The heme binding site, the (putative) methionine ligand, and the histidine ligand are shown in bold. The vertical line indicates the start of the mature proteins. Residues conserved between the heliobacterial cytochrome c_{553} and c_{555}^{m} from *Aquifex* (Mb) and between all of the soluble proteins (Sol) are shown. Italic letters in cytochrome c_{555}^{m} emphasize its high degree of identical residues with respect to cytochrome c_{555}^{s}. Shading indicates α-helical structures (dark gray) and β-sheets (light gray) in the proteins either taken from the structure [TheTh (PDB entry: 1C52), PseSt (PDB entry: 1CCH), HydTh (PDB entry: 1AYG)] or predicted in the modeled structure of cytochrome c_{555}^{s} (AquAe).

showed that the N-terminal fragment corresponds to positions 18−27 of the *cyc*B2 gene (Figure 2). CycB2 consists of 104 amino acid residues with a theoretical molecular weight of 11 600. The heme attachment site CXXCH, typical for *c*-type cytochromes, is located between positions 29 and 32. Two methionine residues, Met-78 and Met-84, are present in the sequence stretch that commonly contains the sixth Met ligand for the heme iron in class I cytochromes (see below). The N-terminal stretch of 17 amino acid residues of the *cyc*B2 gene product, absent in the mature protein, displays the typical features of a signal peptide for translocation across the cytoplasmic membrane into the periplasmic space, i.e., a positively charged N-terminus followed by a hydrophobic region and a signal peptidase cleavage site (*23*). Cleavage of the N-terminal signal peptide in the mature protein argues for a periplasmic localization of this cytochrome. A molecular weight of 9901 is expected for the mature protein in agreement with the apparent molecular weight of CycB2 on SDS−PAGE. Sequence comparisons to a variety of small periplasmic soluble cytochromes revealed significant homology (identity >30%, homology >50%) to cytochromes from other Aquificales (cytochrome c_{552} from *Hydrogenobacter thermophilus*), from the *Deinococcus*/*Thermus* group (cytochrome c_{554} from *T. thermophilus*), and from Firmicutes (cytochrome c_{553} from *Heliobacillus gestii*) as well as from proteobacteria (cytochrome c_{552} from *Nitrosomonas europaea* and cytochrome c_{551} of various *Pseudomonas* strains) (Figure 2). The three-dimensional structures of these cytochromes (for those known) were found to be rather similar to each other (*24*−*27*). The structure of cytochrome c_{555} from *Aquifex* can thus be modeled using cytochrome c_{554} from *Thermus* as template, yielding a similar overall structure for the *Aquifex* cytochrome. Interestingly, no significant conservation is observed in the region around the two methionine residues.

The closest sequence neighbor to CycB2 from *Aquifex* is none of the above-mentioned soluble cytochromes but rather a second cytochrome from the same species, i.e., the *cyc*B1 gene product. CycB2 is in fact 85% identical and 89% homologous to the last two-thirds of the carboxy-terminal end of CycB1 (Figure 2). The *cyc*B1 gene predicts a protein of 166 amino acid residues with a theoretical molecular weight of 19 135.

Properties of Cytochrome c_{555}^{s}

pH Dependence of the Midpoint Redox Potential. A redox midpoint potential of +220 mV was determined by electrochemical redox titration at pH 7 and 20 °C (Figure 3).

The pH dependence of the redox midpoint potential of cytochrome c_{555}^{s}, measured from CV and SWV data, is depicted in Figure 4. The amplitudes of the CV and SWV signals decreased when the pH was increased from 8 to 11 or was decreased from 6 to 3. Signal sizes were partially restored when the pH was raised back or lowered back from 3 or 11 to neutrality, respectively (data not shown). Redox midpoint potential values remained roughly constant in the pH range of 6−8. Above pH 8 and below pH 6, the redox midpoint potential was pH dependent. The alkaline pH dependence was characterized by a p*K* value on the oxidized form of the heme (pK_{ox2}) of 8.4 whereas the acidic region of the E_m vs pH curve could be fitted assuming p*K* values of 4 (pK_{ox1}) and 5.2 (pK_{red}).

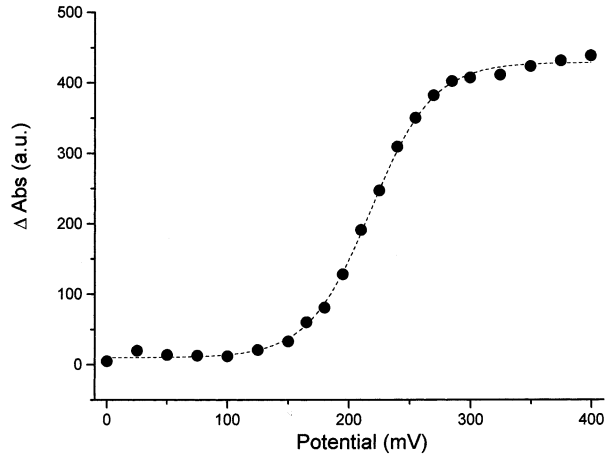

FIGURE 3: Potentiometric titration of the soluble cytochrome c_{555}^{s} from *A. aeolicus*. Electrochemical titration was performed as described in Moss et al. (*11*) without addition of mediators in a buffer containing 50 mM MOPS, pH 7.0, and 100 mM KCl. Spectral amplitude variation was followed in the range of 400 to +600 nm. The data were fitted by an $n = 1$ Nernst curve with a midpoint potential of +220 mV. Reductive and oxidative titrations were superimposable.

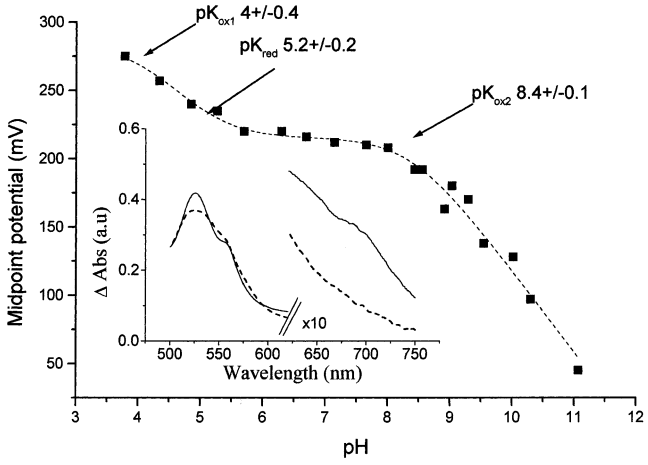

FIGURE 4: pH dependence of the redox midpoint potential of cytochrome c_{555}^{s} from *A. aeolicus*. A buffer mixture of 10 mM sodium acetate/10 mM Tris chloride/10 mM sodium borate was used, and the pH was adjusted to the values indicated. Redox midpoint potentials were determined by both cyclic and square-wave voltammetries as described under Materials and Methods. The obtained results were fitted by the equation (*57*) $E_m = \hat{E} - 0.06 \log[([H^+]^2 + K_{ox1}[H^+] + K_{ox1}K_{ox2})/([H^+]^2 + K_{red}[H^+])]$, where $[H^+]$ is the proton concentration in solution, $\hat{E}$ is the midpoint potential of the fully protonated form, and pK_{ox1} (4 ± 0.4), pK_{red} (5.2 ± 0.2), and pK_{ox2} (8.4 ± 0.1) are three pK values of oxidized and reduced forms. The inset represents optical spectra recorded on cytochrome c_{555}^{s} at pH 7 (straight line) and at pH 10 (dashed line).

pK_{ox} values above 8 in class I cytochromes are frequently associated to loss of methionine coordination of the heme iron (*28*). Optical spectra recorded on oxidized cytochrome c_{555}^{s} at pH 7 and 10 indeed demonstrated a loss of the 695 nm absorption band, commonly attributed to a sulfur iron charge transfer band, i.e., indicative of methionine ligation (inset in Figure 4). This suggests that, like many other class I cytochromes, cytochrome c_{555}^{s} undergoes ligand changes at high pH values.

The pK_{ox1} and pK_{red} values (4 and 5.2, respectively), characterizing the pH dependence beyond neutrality, are separated by approximately one pH unit. A similar pH dependence of the redox midpoint potential was determined for the *Rhodomicrobium vannielii* and *Rhodospirillum rubrum* cytochromes c_2 (*28*). The pK_{ox1} and pK_{red} values are in these cases associated to the ionization of the rear heme propionate. The precise values of pK_{ox} and pK_{red} are proposed to depend on the nature of the residues interacting with the propionate oxygens (*28*).

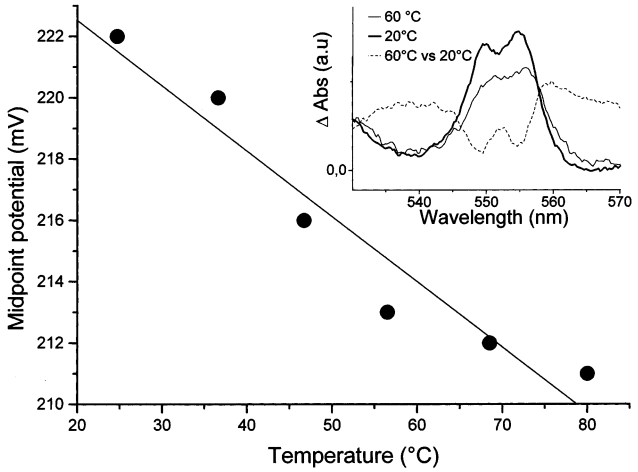

FIGURE 5: Temperature dependence of the redox midpoint potential. Redox midpoint potentials were determined, as described in Materials and Methods, by cyclic and square-wave voltammetries. A straight line characterized by a temperature coefficient $dE^{\circ\prime}/dT$ of −0.2 mV·K^{-1} corresponding to a standard entropy change $S^{\circ\prime}$ of −19 J·mol^{-1}·K^{-1} was fitted to the data points. Spectra recorded on cytochrome c_{555}^{s} at 20 °C (broad line) and 60 °C (dashed line) as well as the difference between these two spectra (dotted line) are shown in the inset.

Temperature Dependence of the Redox Midpoint Potential. Two series of measurements were performed using CV and SWV techniques, either with or without renewing the sample at each investigated temperature. Very similar results were gained from both series of experiments. The temperature dependence of $E_{m,7}$ is shown in Figure 5. The obtained curve yields a temperature coefficient $dE_{m,7}/dT$ of −0.2 mV·K^{-1}. The split α-band observed at 20 °C changed its form when temperature was increased (inset in Figure 5), both absorption bands shifting and overlapping.

EPR Spectroscopy. The EPR spectrum of the oxidized form of cytochrome c_{555}^{s} was characteristic of a low-spin heme with signals at $g_z = 2.89$, $g_y = 2.287$, and $g_x = 1.52$ (Figure 6, panel a).

Properties of Membrane-Bound Cytochrome c_{555}

Optical and EPR spectra recorded on membranes from *A. aeolicus* demonstrated the presence of a cytochrome with optical (spectrum b in Figure 1) and EPR (panel b in Figure 6) parameters similar to those of cytochrome c_{555}^{s}. Both the optical and EPR spectra of this cytochrome persisted even in membranes treated with chaotropic agent. This suggested that the respective cytochrome was indeed tightly attached to the membrane and was distinct from cytochrome c_{555}^{s}. We therefore refer to this heme protein in the following as cytochrome c_{555}^{m}. Redox titration of the $g_z = 2.88$ EPR signal of cytochrome c_{555}^{m} in membrane fragments yielded a midpoint redox potential of +210 ± 20 mV ($n = 1$) (Figure 7).

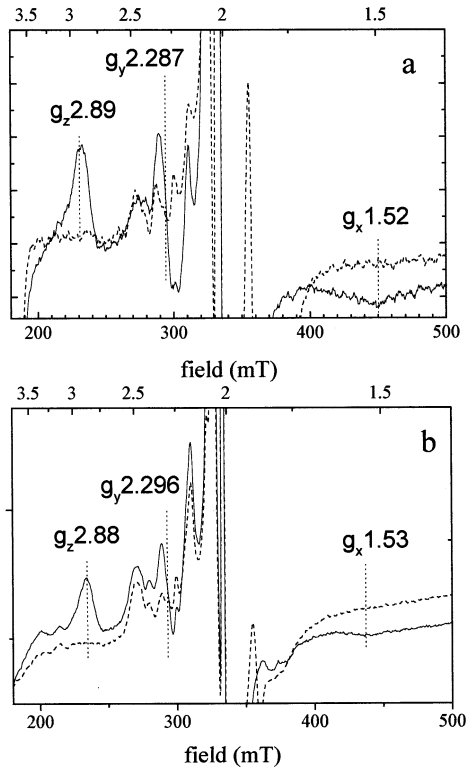

FIGURE 6: EPR spectra of the soluble (panel a) and the membrane-attached (panel b) c_{555} cytochromes. Spectra were recorded on samples without addition (straight line) or treated with 5 mM ascorbate (dashed line). g_x, g_y, and g_z values for cytochrome c_{555}^{s} were determined at 1.52, 2.287, and 2.89, respectively, whereas they were found at 1.53, 2.296, and 2.88, respectively, for the membrane-attached cytochrome c_{555}^{m}.

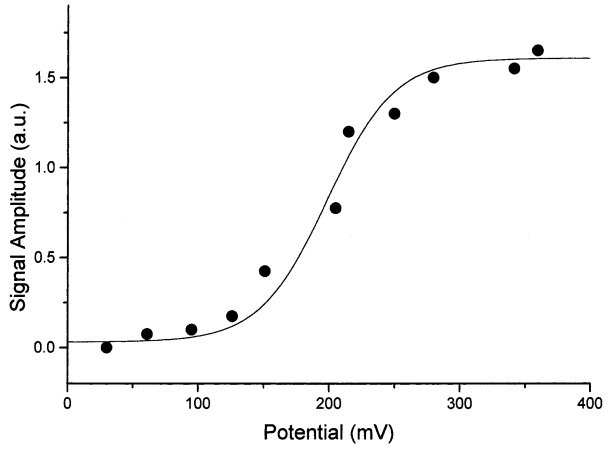

FIGURE 7: EPR titration of the membrane-attached cytochrome c_{555}^{m}. Titrations were performed in a buffer containing 50 mM MOPS, pH 7.0, 2 mM EDTA, and 40 mM NaCl in the presence of redox mediators as indicated in Materials and Methods. The titration curve represents the dependence of the $g_z = 2.88$ signal size on ambient redox potential. The data points were fitted by an $n = 1$ Nernst curve assuming a redox midpoint potential of +210 mV.

EPR Experiments on Partially Ordered Membrane Fragments. EPR spectra were recorded on oriented, untreated (i.e., largely oxidized) membranes of *A. aeolicus* in a range of angles between −80° to +90° (magnetic field with respect to the plane of the membrane) (Figure 8a). The sample was well ordered as judged from the strong anisotropy of the g_z peak at $g = 3.03$, attributed to heme *a* of the cytochrome aa_3 oxidase (to be published) (Figure 8b, open circles). In

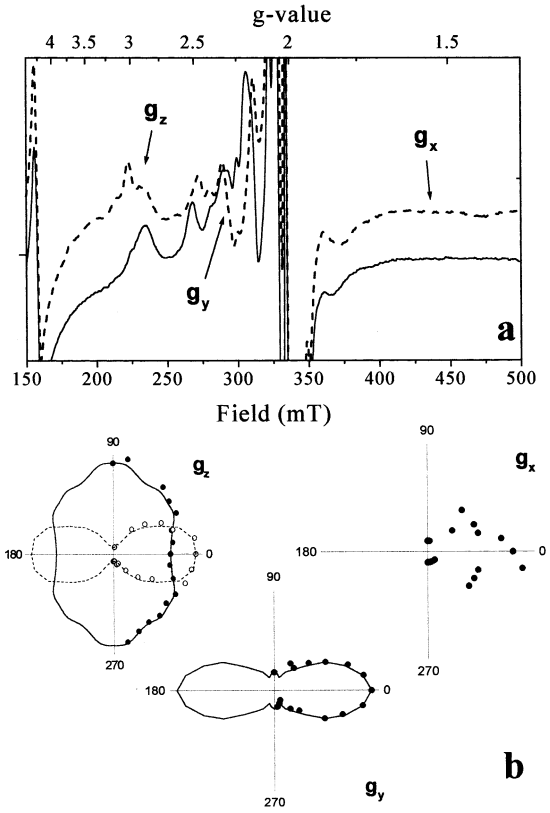

FIGURE 8: EPR study of two-dimensionally ordered membrane fragments. Panel a: EPR spectra recorded on oriented membrane multilayers prepared according to Rutherford and Sétif (*13*) without adding exogenous oxidant or reductant and exposed to air. Under these conditions, redox centers with E_m values below +300 mV were found to be largely oxidized. The magnetic field was oriented 90° (straight line) or 0° (dashed line) with respect to the plane of the membrane. The peak at $g = 2.88$ corresponds to the g_z line of cytochrome c_{555}^{m} and that at $g = 3.03$ is attributed to cytochrome oxidase. Panel b: Polar plot evaluation of the signal amplitudes of the g_z peaks arising from cytochrome oxidase (open circles) and from cytochrome c_{555}^{m} (closed circles) as well as the g_x and g_y lines of cytochrome c_{555}^{m}.

contrast to this signal (and several others that are not shown), the orientation dependence of the $g_z = 2.88$ line intensity (attributed to cytochrome c_{555}^{m}) showed multiple maxima. A polar plot evaluation of the $g_z = 2.88$ signal amplitude (closed circles in Figure 8b) indicates three weak maxima at 30°, 50°, and 80° with respect to the membrane. The polar plot evaluation of the intensity of the $g_x = 1.53$ trough, although less accurate due to lower signal-to-noise ratio, also indicated several maxima.

DISCUSSION

Phylogenetic Analysis. BLAST searches in sequence databases for homologous proteins yielded predominantly class I *c*-type cytochromes, such as the small soluble cytochromes from several proteobacteria, from the Aquificalis *H. thermophilus*, or from *T. thermophilus* as well as the membrane-attached cytochrome c_{553} from *H. gestii*.

A multiple alignment of the retrieved sequences was performed with the help of CLUSTAL X, and phylogenetic trees were calculated using the Neighbor-Joining method. It is noteworthy that the N-terminal extension of the membrane-attached heme proteins cytochrome c_{555}^{m} from *A. aeolicus* and cytochrome c_{553} from *H. gestii* was not taken into account

in this analysis. The obtained trees varied slightly in topological details, presumably due to the restricted number of sites in these very small proteins. A few aspects, however, were common to all calculated trees and are therefore worth mentioning. (i) Both *Aquifex* cytochromes form a clade (bootstrap of 100) showing that the presence of two cytochromes c_{555} is due to gene duplication in the Aquificales. (ii) The *A. aeolicus* cytochromes c_{555} cluster with the heliobacterial cytochrome c_{553} (it is noteworthy that this does not result from a bias conferred by the N-terminal extension which was omitted from the analysis). The substantial sequence homology of the N-terminal extension (Figure 2) together with this phylogenetic proximity of the C-terminal heme domains indicates that the parent gene in *A. aeolicus* was probably that of the membrane-attached cytochrome $c_{555}{}^{m}$. Gene duplication and N-terminal truncation may then have resulted in the soluble cytochrome $c_{555}{}^{s}$. (iii) Cytochrome c_{555} from *A. aeolicus*, cytochrome c_{553} from *H. gestii*, and cytochrome c_{554} from *T. thermophilus* form a clade which is well separated from that containing the proteobacterial cytochromes and cytochrome c_{552} from *H. thermophilus*. There are several reports in the literature showing that *A. aeolicus* contains a substantial number of genes related to proteobacterial ones (*7*), and it was proposed that *Aquifex* has experienced extensive lateral gene transfer from a proteobacterial donor (*6*). A recent analysis suggests that about 20% of the *A. aeolicus* genome represents genes related to proteobacteria (Brugna and Nitschke, unpublished). Since the *Aquifex* cytochromes do not cluster together with the proteobacterial counterparts, these two heme proteins may in fact be part of the genuine heritage of the Aquificales lineage. (iv) The *Hydrogenobacter* cytochrome, by contrast, was found to cluster with the proteobacterial proteins in all trees obtained. This would indicate that the Aquificalis *H. thermophilus* uses a proteobacterial gene to code for its soluble cytochrome whereas *A. aeolicus* employs a lineage-related protein. In the model of lateral gene transfer into the Aquificales mentioned above, this would mean that either *H. thermophilus* has acquired its cytochrome c_{552} gene after the branching off of *A. aeolicus* or that the common ancestor of *H. thermophilus* and *A. aeolicus* contained both lines of cytochromes, one or the other of which was lost in the descendent species.

Adaptation to Hyperthermophilic Conditions. The determination of the factors leading to thermostability represents a major goal in the study of thermo- and hyperthermophilic organisms. For the particular case of a mesophilic representative of the small soluble class I *c*-type cytochromes, site-directed mutagenesis guided by sequence and structure comparisons with its thermophilic homologue in the Aquificalis *H. thermophilus* has recently succeeded in confering thermostability to this cytochrome, thereby showing that the modification of only a few selected residues can result in thermostability (*29*). As mentioned above, the *Hydrogenobacter* cytochrome appears to be phylogenetically closely related to its proteobacterial counterparts. A straightforward comparison between these proteins was therefore possible. The equivalent approach is not possible for the case of both *Aquifex* cytochromes c_{555}. The determination of the 3D structure of at least one of these two cytochromes and a subsequent comparison of sequence and structural characteristics between the proteobacterial and the *Hydrogenobacter* cytochromes on one side and the *Thermus* and *Aquifex* cytochromes on the other side may therefore provide more profound insight into the parameters distinguishing between meso- (<45 °C), thermo- (45−80 °C), and hyperthermostable (>80 °C) proteins. Overproduction of the *A. aeolicus* cytochromes in *E. coli* has therefore been initiated [see accompanying article (*58*)] as a crucial prerequisite to ultimately determine the structure.

In the native soluble cytochrome $c_{555}{}^{s}$ from *A. aeolicus*, the dependence of the redox midpoint potential on temperature was examined. The E_m was found to be only weakly dependent on *T*, amounting to a total change of 12 mV in the range from 20 to 80 °C. The deduced entropy contribution turned out to be relatively low as compared to that of meso- and thermophilic proteins (*17*, *30*, *31*). The constant slope of the E_m vs *T* curve in the region explored furthermore showed that no major conformational changes occur in this temperature range. Thermostability parameters of the heterologously expressed protein and mutants thereof are described in the accompanying article (*58*).

Two Possible Candidates for the Sixth Ligand Methionine. The positioning of the *c*-heme attachment motif (CXXCH) in the N-terminal region of the sequence and of the methionine residues putatively serving as the sixth heme ligand approximately 40 residues further toward the C-terminal end suggested that both cytochromes c_{555} belong to the class I *c*-type cytochromes. Following Ambler's classification scheme (*32*), the presence of a M...LS...I motif downstream of the methionine ligand as well as of a split α-band defines the cytochromes c_{555} as representatives of the subclass Ic.

Unlike most class I cytochromes, two different methionine residues (five and six residues apart in the cytochrome $c_{555}{}^{m}$ and cytochrome $c_{555}{}^{s}$ sequences, respectively) are present in the sequence stretch typically harboring the sixth ligand methionine. In proteobacterial class I cytochromes, the second residue after the ligating methionine frequently is a proline. On the basis of the presence of such a proline following the first of the two methionines in both *Aquifex* cytochromes, this first methionine was aligned with the sixth ligand of the proteobacterial proteins. Interestingly, however, two methionines, six residues apart, are also present in cytochrome c_{554} from *T. thermophilus*. The crystal structure of the *Thermus* cytochrome has been solved (*27*), showing that the second of the two Met residues is the axial ligand. This second methionine was consequently aligned with the ligating Met of the class I proteobacterial cytochromes in Figure 2. Since homology in this sequence region between the proteins from *Aquifex*, *Thermus*, and the proteobacteria is low, an alignment of the two respective Met residues of *Aquifex* and *Thermus* is equally possible. Such an alignment would suggest the second Met residue in the *Aquifex* proteins as the heme ligand. Sequence comparisons alone therefore did not allow us to unequivocally identify the methionine serving as the sixth ligand in the *A. aeolicus* cytochromes. This question was therefore addressed by site-directed mutagenesis, and the respective results are presented in the accompanying article (*58*).

Cellular Localization of Both Cytochromes and Mode of Membrane Attachment of Cytochrome $c_{555}{}^{m}$. The N-terminal sequence of the mature form of cytochrome $c_{555}{}^{s}$ was determined, demonstrating that the first 17 amino acid

residues of the gene product represent a cleaved-off leader peptide. The characteristics of this leader peptide suggested that it serves in translocation of cytochrome c_{555}^{s} into the periplasmic space. The sequence of the 17-residue leader peptide of cytochrome c_{555}^{s} is strongly conserved in the gene sequence of cytochrome c_{555}^{m}, suggesting that also this latter heme protein is addressed to the periplasmic space. In contrast to its soluble counterpart, cytochrome c_{555}^{m} fractionated with the membrane and even treatment of membranes with chaotropic salts did not liberate any soluble form of cytochrome c_{555}^{m}, indicating a strong association of this heme protein to the lipid bilayer. This raised the question of the mode of anchoring of cytochrome c_{555}^{m} to the membrane. The astonishingly high homology of the C-terminal part of cytochrome c_{555}^{m}'s amino acid sequence to that of its soluble counterpart suggests that membrane attachment is mediated by the N-terminal extension of cytochrome c_{555}^{m}. Apart from the supposed leader peptide, no hydrophobic stretch could be identified in this N-terminal extension. A clue to the probable mode of membrane attachment came from the significant sequence homology of cytochrome c_{555}^{m} to cytochrome c_{553} from *H. gestii*. Heliobacterial cytochrome c_{553} has been shown to be a lipoprotein with the lipid residues presumably attached to an N-terminal Cys residue in the mature protein (33). Intriguingly, a Cys residue is present in cytochrome c_{555}^{m} from *A. aeolicus* immediately following the first 17 amino acid residues supposed to be a leader peptide. These residues including the Cys aligned very well with the residues in *H. gestii* cytochrome c_{553}. We therefore propose that cytochrome c_{555}^{m} from *Aquifex* also is a lipoprotein. Confirmation of this hypothesis and a more detailed characterization of the lipid molecules require purification of sufficient quantities of cytochrome c_{555}^{m} from the membrane fraction, which has not been achieved so far. If this model is correct, *A. aeolicus* cytochrome c_{555}^{m} represents one more exception (see also refs *33* and *34*) to the previously stipulated rule of lipoproteins being characterized by a LAGC/LAAC signal peptide sequence necessary for binding of the signal peptidase (*23*).

Cytochrome c_{555}^{m} Belongs to the Family of Pivoting Cytochromes. The described EPR results obtained on partially ordered membrane multilayers showed that the cytochrome c_{555}^{m} heme can adopt several (or possibly even a continuum of) orientations with respect to the membrane. This indicated that the membrane extrinsic domain of cytochrome c_{555}^{m} performs pivoting movements on the membrane surface. The obtained results are reminiscent of those obtained by EPR on the Rieske protein in cytochrome *bc* complexes (*35*−*38*) and in particular of those described for another membrane-attached cytochrome, i.e., cytochrome $b_{558/566}$ from the Archaeon *Sulfolobus acidocaldarius* (*39*). Whereas for the case of the *Sulfolobus* cytochrome $b_{558/566}$ only the g_z value was detected, the orientations of all three principal *g*-tensor directions could be observed for cytochrome c_{555}^{m}. Multiple maxima were seen for g_z whereas the g_y direction displayed a single and well-defined maximum parallel to the membrane plane. In the limit of the poor signal-to-noise ratio, the g_x signal also appeared to show more than one maximum. A straightforward rationalization of these observations consists of assuming that the g_y axis is close to the rotation axis of the protein and that the conformational motion would therefore be restricted and guided rather than represent a mere "dangling" of the extrinsic domain from the membrane surface. At the present time, however, this interpretation should be taken with caution. Whereas for paramagnetic centers with a fixed conformation the observed g directions always form an orthonormal set (*40*), this rule does not seem to hold for the case of "mobile-domain" centers (*36*, *38*). A possible explanation for this phenomenon consists of assuming variable population densities along the different *g* axes. For instance, a given conformational substate may be well-ordered along one *g* direction, correspondingly leading to an intense EPR signal, but relatively disordered along one or both of the remaining directions, resulting in weak signals possibly difficult to distinguish in a polar plot. A quantitative evaluation of the polar plot dependences in these wobbling centers is therefore not possible at this time. Computational simulations of the experimental polar plots might help to remediate this problem, and we are therefore presently initiating efforts in this direction.

The possibility of domain movement in membrane-attached cytochromes was evoked as early as 1979 for the case of liver microsomal cytochrome b_5 (*41*). More recently, sequence and kinetic data on cytochrome c_y from *Rhodobacter capsulatus* indicated a respective flexibility for this heme protein (*42*−*44*). Close relatives of cytochrome c_y have subsequently been identified in several proteobacterial species (*45*−*47*). Kinetic arguments in favor of the possibility of domain movements have also been reported for cytochrome c_z in green sulfur bacteria (*48*). A comparable domain flexibility was proposed for membrane-attached cytochromes in Bradyrizobia (*45*) and Gram-positive bacteria (*49*).

In the case of the c_y cytochromes, the extrinsic heme binding domain is linked to the membrane anchor via a stretch of 43−61 amino acid residues (*45*−*47*, *50*). In *A. aeolicus* cytochrome c_{555}^{m}, 62 residues connect the domain homologous to cytochrome c_{555}^{s} to the presumable N-terminal lipid anchor. Current prediction algorithms did not yield an evident secondary structure for this sequence stretch, and it can therefore not be decided at present whether this stretch merely acts as a leash or whether it is folded into a specific structure.

Several of the mentioned cytochromes are parts of larger enzyme supercomplexes. The cytochromes c_{552} from *Paracoccus denitrificans* and c_{551} from *Bacillus* PS3, for example, are integrated into a supercomplex additionally containing the cytochrome *bc* complex and cytochrome oxidase (*49*, *51*). At present, we do not know whether cytochrome c_{555}^{m} represents an isolated membrane-attached heme protein or whether it is part of a larger entity. Purification attempts are in progress to address this question.

Functional Role of the Two Cytochromes c_{555}. No direct evidence concerning the functional roles of cytochrome c_{555}^{s} and cytochrome c_{555}^{m} in *A. aeolicus* has been obtained so far. Their redox midpoint potentials suggest that one or both might be involved in electron transfer from the cytochrome *bc* complex toward terminal oxidases similar to the task fulfilled by cytochrome c_y in proteobacteria. In such a scenario, the two different cytochromes may either be specific to different electron transfer pathways or act as competing or successive carriers in the same chain. In the case of *R. capsulatus* for example, the soluble and membrane-bound counterparts have both competing functions in the cytochrome bc_1/aa_3 oxidase chain (*44*, *52*) but different

specific functions in the nitrous and nitric oxide reductase activity, respectively (*53*, *54*). In this context, it seems noteworthy to us that none of the other species studied so far contains two cytochromes with so similar properties (with respect to sequence, redox midpoint potential, and optical and EPR spectra). Whereas this may admittedly represent a rather recent gene duplication, it could also reflect functional constraints requiring conservation of the extrinsic domain. Cytochrome c_{555}^{s} has a tendency to associate into multimeric forms influencing both redox and optical properties (data not shown). The similarity between the heme binding domains of cytochrome c_{555}^{m} and cytochrome c_{555}^{s} may suggest interaction between the two proteins. Such a heterologous association could create an electron transfer couple as reported for the diheme cytochrome c_4 (*55*) or for the dimeric cytochrome c_{552} from *Pseudomonas nautica* (*56*).

A dynamic analysis of the *Aquifex* electron transfer chain and the identification of possible supercomplex formation between the enzymes involved may help to further elucidate the detailed functional role of the two c_{555} cytochromes.

ACKNOWLEDGMENT

We thank R. Huber (Regensburg, FRG) for providing cell material of *Aquifex aeolicus*. We also thank the group of P. Bertrand (Marseille, France) for extensive access to their EPR equipment.

REFERENCES

1. Huber, R., Wilham, T., Huber, D., Trincone, A., Burggraf, S., König, H., Rachel, R., Rockinger, I., Fricke, H., and Stetter, K. O. (1992) *Syst. Appl. Microbiol. 15*, 340−351.
2. Olsen, G. J., Woese, C. R., and Overbeek, R. (1994) *J. Bacteriol. 176*, 1−6.
3. Deckert, G., Warren, P. V., Gaasterland, T., Young, W. G., Lenox, A. L., Graham, D. E., Overbeek, R., Snead, M. A., Keller, M., Aujay, M., Huber, R., Feldman, R. A, Short, J. M., Olsen, G. J., and Swanson, R. V. (1998) *Nature 392*, 353−358.
4. Yeh, A. P., Chatelet, C., Soltis, S. M., Kuhn, P., Meyer, J. and Rees, D. C. (2000) *J. Mol. Biol. 14*, 587−595.
5. Nübel, T., Klughammer, C., Huber, R., Hauska, G., and Schütz, M. (2000) *Arch. Microbiol. 173*, 233−244.
6. Schütz, M., Brugna, M., Lebrun, E., Baymann, F., Huber, R., Stetter, K.-O., Hauska, G., Toci, R., Lemesle-Meunier, D., Tron, P., Schmidt, C., and Nitschke, W. (2000) *J. Mol. Biol. 300*, 663−675.
7. Klenk, H. P., Meier, T. D., Durovic, P., Schwass, V., Lottspeich, F., Dennis, P. P., and Zillig, W. (1999) *J. Mol. Evol. 48*, 528−541.
8. Nelson, K. E., Clayton, R. A., Gill, S. R., Gwinn, M. L, Dodson, R. J., Haft, D. H., Hickey, E. K., Peterson, J. D., Nelson, W. C., Ketchum, K. A., McDonald, L., Utterback, T. R., Malek, J. A., Linher, K. D., Garrett, M. M., et al. (1999) *Nature 399*, 323−329.
9. Snel, B., Bork, P., and Huyen, M. A. (1999) *Nat. Genet. 21*, 108−110.
10. Dutton, P. L. (1971) *Biochim. Biophys. Acta 226*, 63−80.
11. Moss, D. A., Nabedryk, E., Breton, J., and Mäntele, W. (1990) *Eur. J. Biochem. 187*, 565−572.
12. Blasie, J. K., Erecinska, M., Samuels, S., and Leigh, J. S. (1978) *Biochim. Biophys. Acta 501*, 33−52.
13. Rutherford, A. W., and Sétif, P. (1990) *Biochim. Biophys. Acta 1019*, 128−132.
14. Osteryoung, J., and O'Dea, J. J. (1986) in *Electroanalytical Chemistry: A Series of Advances* (Bard, A. J., Ed.) Vol. 14, pp 209−110, Marcel Dekker, New York.
15. Haladjian, J., Bianco, P., Nunzi, F., and Bruschi, M. (1994) *Anal. Chim. Acta 289*, 15−20.
16. Taniguchi, I., Toyosawa, K., Yamaguchi, H., and Yasukouchi, K. (1982) *J. Chem. Soc., Chem. Commun.*, 1032.
17. Taniguchi, V. T., Sailasuta-Scott, N., Anson, F. C., and Gray, H. B. (1980) *Pure Appl. Chem. 52*, 2275.
18. Laemmli, U. K. (1970) *Nature 227*, 680−685.
19. Thomas, P. E., Ryan, D., and Levin, W. (1976) *Anal. Biochem. 75*, 168−176.
20. Altschul, S. F., Gish, W., Miller, W., Myers, E. W., and Lipman, D. J. (1990) *J. Mol. Biol. 215*, 403−410.
21. Thomson, J. D., Gilson, T. J., Plewniak, F., Jeanmougin, F., and Higgins, D. G. (1997) *Nucleic Acids Res. 24*, 4876−4882.
22. Guex, N., and Peitsch, M. C. (1997) *Electrophoresis 18*, 2714−2723.
23. von Heijne, G. (1988) *Biochim. Biophys. Acta 947*, 307−333.
24. Timkovich, R., Bergmann, D., Arciero, D. M., and Hooper, A. B. (1998) *Biophys. J. 75*, 1964−1972.
25. Cai, M., and Timkovich, R. (1994) *Biophys. J. 67*, 1207−1215.
26. Hasegawa, J., Yoshida, T., Yamazaki, T., Sambongi, Y., Yu, Y., Igarashi, Y., Kodama, T., Yamazaki, K.-I., Kyogoku, Y., and Kobayashi, Y. (1998) *Biochemistry 37*, 9641−9649.
27. Than, M. E., Hof, P., Huber, R., Bourenkov, G. P., Bartunik, H. D., Buse, G., and Soulimane, T. (1997) *J. Mol. Biol. 271*, 629−644.
28. Moore, G. R., and Pettigrew, G. W. (1990) in *Cytochromes c. Evolutionary, structural and physicochemical aspects*, Springer-Verlag, Berlin.
29. Hasegawa, J., Uchiyama, S., Tanimoto, Y., Mizutani, M., Kobayashi, Y., Sambongi, Y., and Igarashi, Y. (2000) *J. Biol. Chem. 275*, 37824−37828.
30. Verhagen, M. F. J. M., Wolbert, R. B. G., and Hagen, W. R. (1994) *Eur. J. Biochem. 221*, 821−829.
31. Florens, L., Bianco, P., Haladjian, J., Bruschi, M., Protasevich, I., and Makarov, A. (1995) *FEBS Lett. 373*, 280−284.
32. Ambler, R. P. (1991) *Biochim. Biophys. Acta 1058*, 42−47.
33. Albert, I., Rutherford, A. W., Grav, H., Kellermann, J., and Michel, H. (1998) *Biochemistry 37*, 9001−9008.
34. Weyer, K. A., Schäfer, M., Lottspeich, F., and Michel, H. (1987) *Biochemistry 26*, 2909−2914.
35. Brugna, M., Albouy, D., and Nitschke, W. (1998) *J. Bacteriol. 180*, 3719−3723.
36. Schoepp, B., Brugna, M., Riedel, A., Nitschke, W., and Kramer, D. (1999) *FEBS Lett. 450*, 245−251.
37. Brugna, M., Nitschke, W., Asso, M., Guigliarelli, B., Lemesle-Meunier, D., and Schmidt, C. (1999) *J. Biol. Chem. 274*, 16766−16772.
38. Brugna, M., Rodgers, S., Schriker, A., Montoya, G., Kazmeier, M., Nitschke, W., and Sinning, I. (2000) *Proc. Natl. Acad. Sci. U.S.A. 97*, 2069−2074.
39. Schoepp-Cothenet, B., Schütz, M., Baymann, F., Brugna, M., Nitschke, W., Myllykallio, H., and Schmidt, C. (2001) *FEBS Lett. 487*, 372−376.
40. Hootkins, R., and Bearden, A. (1983) *Biochim. Biophys. Acta 723*, 16−29.
41. Rich, P. R., Tiede, D. M., and Bonner, W. D., Jr. (1979) *Biochim. Biophys. Acta 546*, 307−315.
42. Prince, R. C., Davidson, E., Haith, C. E., and Daldal, F. (1986) *Biochemistry 25*, 5208−5214.
43. Jenney, F. E., Prince, R. C., and Daldal, F. (1994) *Biochemistry 33*, 2496−2502.
44. Myllikallio, H., Drepper, F., Mathis, P., and Daldal, F. (1998) *Biochemistry 37*, 5501−5510.
45. Bott, M., Ritz, D., and Hennecke, H. (1991) *J. Bacteriol. 173*, 6766−6772.
46. Turba, A., Jetzek, M., and Ludwig, B. (1995) *Eur. J. Biochem. 231*, 259−265.
47. Myllykallio, H., Zannoni, D., and Daldal, F. (1999) *Proc. Natl. Acad. Sci. U.S.A. 96*, 4348−4353.
48. Oh-oka, H., Iwaki, M., and Itoh, S. (1997) *Biochemistry 36*, 9267−9272.
49. Sone, N., Sekimashi, M., and Kutoh, E. (1987) *J. Biol. Chem. 262*, 15386−15391.

50. Myllykallio, H., Jenney, F. E., Moomaw, C. R., Slaughther, C. A., and Daldal, F. (1997) *J. Bacteriol. 179*, 2623−2631.
51. Berry, A. E, and Trumpower, B. L. (1985) *J. Biol. Chem. 260*, 2458−2467.
52. Hochkoeppler, A., Jenney, F. E., Lang, S. E., Zannoni, D., and Daldal, F. (1995) *J. Bacteriol. 177*, 608−613.
53. Richardson, D. J., Bell, L. C., MaEwan, A. G., Jackson, J. B., and Ferguson, S. J. (1991) *Eur. J. Biochem. 199*, 677−683.
54. Bell, L. C., Richardson, D. J., and Ferguson, S. J. (1992) *J. Gen. Microbiol. 138*, 437−443.
55. Kadziola, A., and Larsen, S. (1997) *Structure 5*, 203−216.
56. Brown, K., Nurizzo, D., Besson, S., Shepard, W., Moura, J., Moura, I., Tegoni, M., and Cambillau, C. (1999) *J. Mol. Biol. 289*, 1017−1028.
57. Clark, W. M. (1960) in *Oxidation Reduction Potential of Organic Systems*, Williams and Wilkins, Baltimore, MD.
58. Aubert, C., Guerlesquin, F., Bianco, P., Leroy, G., Tron, P., Stetter, K.-O., and Bruschi, M. (2001) *Biochemistry 40*, 13690−13698.

BI011201Y